

Figure S1 : Effect of heterogeneous synaptic weights and synaptic waveform on the power law frequency scaling exponent. **A-B** V_m frequency-scaling exponent changes for different input frequencies ν and for heterogeneous synaptic strengths. The synaptic strengths are randomly distributed for each incoming synaptic spike train according to a gaussian law whose standard deviation is half the mean value in this case. These controls have been performed with integrate-and-fire neurons (panel A), Hodgkin-Huxley neurons (panel B). Synchrony percentage is kept a 6% and there is no correlation between excitatory and inhibitory synaptic inputs. Error bars are the standard deviation over the trials. The bold line represents the average across cells and trials. **C-D** Variation of the value of the frequency-scaling exponent at the membrane potential level for excitatory input only as a function of the parameters β_{exc} and for β -synapses ($r = 3\%$). **A** Illustration of the PSD modulation in a log-log scale for different values of the parameter β_{exc} ranging from 0 (light blue) to 1 (dark blue). In the inset, a stereotypic synaptic time course is represented (with a time rise of 1 ms). **B** Variation of the output frequency-scaling exponent with the β_{exc} parameter.

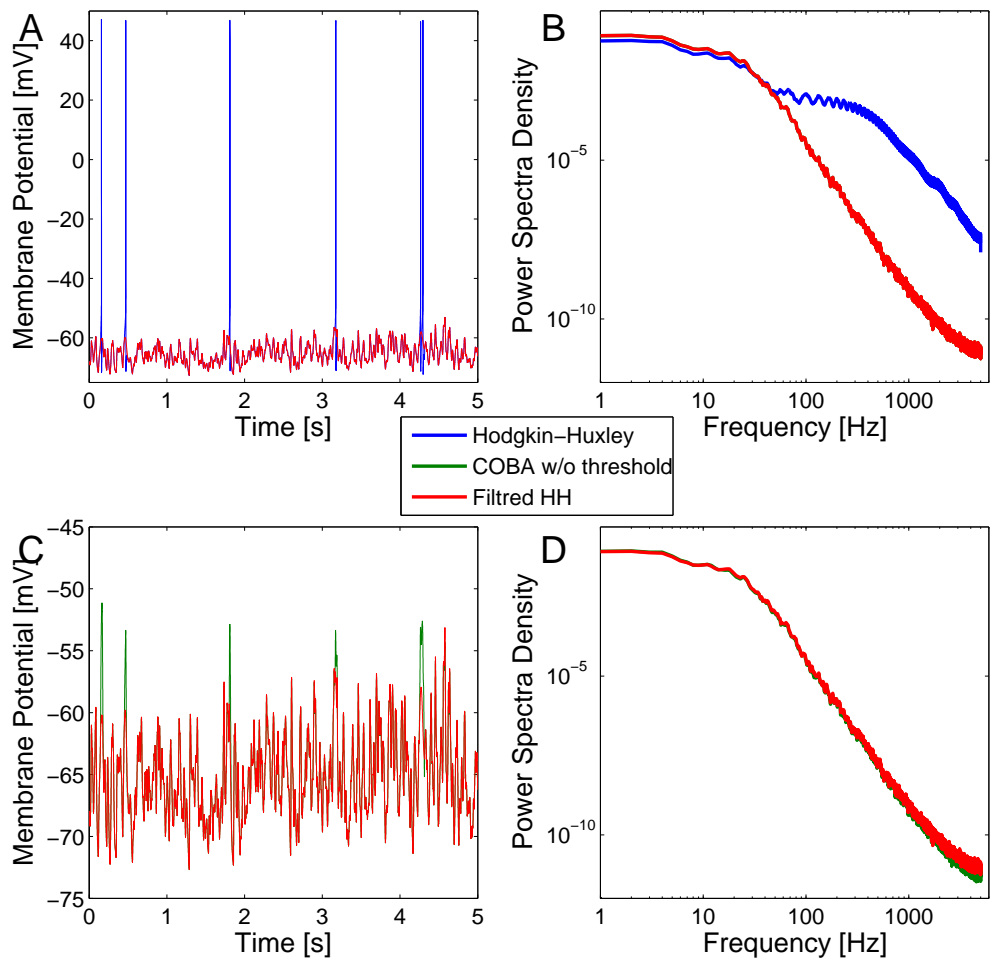


Figure S2 : Illustration of the spike filtering algorithm for neuron models with and without spiking mechanism. **A** Injection of correlated synaptic input to a HH model. Blue: raw trace ; Red: after spike filtering. **B** Power spectra density corresponding to **A**. **C** injection of the same synaptic input in a COBA model without threshold (green), superimposed to the HH-spike-filtered trace plotted in **A**. **D** Power spectra density of the the two traces displayed in **C** : COBA without threshold and HH with spike filtered.

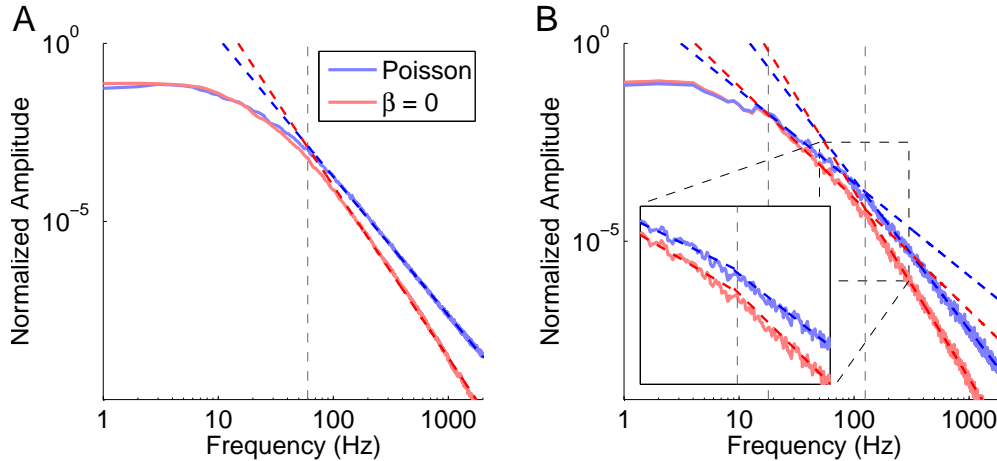


Figure S3 : Influence of the different integrative time constants on the PSD frequency scaling. **A**: V_m power spectra for different levels of correlation in the input (blue: Poisson input ; red: correlated input with $k = 6\%$ and $\beta = 0$). The level of conductance is low in this condition ($G_{\text{tot}} = 0.23G_{\text{leak}}$). The dotted coloured lines indicate the linear fits over the high frequency region delimited by the vertical dashed gray line. **B**: same PSD, but for a very high conductance state ($G_{\text{tot}} = 12G_{\text{leak}}$). The four fits correspond to fit in different frequency bands, for the two PSDs.

To illustrate more precisely the differential effect of the conductance state and of the input correlations on the frequency-scaling exponent, we show several examples of V_m power spectra for two different levels of global conductance regime, and two different $\beta_{\text{inh}} = \beta_{\text{exc}}$ parameters. In the low conductance state (A), the power spectrum is composed of two linear regions separated by a unique cut-off, which is determined by the time constants of the synaptic and membrane filtering. In the very high conductance state (B), these two time constants are clearly different. So the power spectrum shows three linear regions separated by two cut-offs. Very large (and surely not plausible in biological conditions) changes of the conductance state thus displaced the second frequency cut-off, but still did not affect the relative slope in the linear regions. Decreasing the β parameter increases the slope over both frequency bands and relative changes of the frequency-scaling exponent have the same magnitude in these different regions. This shows that the relative modulation observed is not dependent on the specific frequency band chosen to estimate the PSD slope, since it can be observed over a large range of frequencies. Furthermore, this figure illustrates the differential effect of the conductance state, and of the correlation state, on the power spectrum. Opposite to the latter, the former does not affect the scaling exponent.

Layer III cell	HC	LC	VLC
$r = 0\%$	3.40	3.39	3.38
$r = 1.5\%$	3.56	3.62	3.63
Layer VI cell	HC	LC	VLC
$r = 0\%$	3.39	3.36	3.29
$r = 1.5\%$	3.54	3.55	3.51

Table S1 : Frequency-scaling exponents for detailed neuron models. Neuron models were obtained from neuronal morphologies reconstructed from a layer III cell (upper table) and a layer VI cell (lower table) of the cat cerebral cortex (see methods). The frequency-scaling exponent is computed for different synaptic input firing rates and different levels of synchrony. Three levels of incoming synaptic activity have been considered, following (Destexhe and Paré, 1999) : a high-conductance state (HC) with $\nu_{\text{exc}} = 1$ Hz, $\nu_{\text{inh}} = 5.5$ Hz; a low-conductance state (LC) with $\nu_{\text{exc}} = \nu_{\text{inh}} = 0.5$ Hz and a very low-conductance state (VLC) with $\nu_{\text{exc}} = \nu_{\text{inh}} = 0.1$ Hz. Each condition was performed with two levels of synchrony between synaptic spike trains, $r = 0\%$ and $r = 1.5\%$ respectively. Frequency-scaling exponents barely changed with the increasing firing rate for uncorrelated inputs and the correlated case for both cells. On the contrary, the frequency-scaling exponent was affected by the level of synchrony, as expected by our previous results. These simulations show that the relative modulation of the scaling exponent are well captured by correlation changes, while conductance changes have a negligible effect.

References

Destexhe A, Paré D (1999) Impact of network activity on the integrative properties of neocortical pyramidal neurons in vivo. *J Neurophysiol* 81: 1531–1547.